Received: 13 April 2022 | Revised: 12 October 2022 | Accepted: 22 October 2022

DOI: 10.1002/da.23295

RESEARCH ARTICLE

ANXIETY AND DEPRESSION ASSOCIATION OF AMERICA WILEY

Elucidating behavioral and functional connectivity markers of aberrant threat discrimination in PTSD

John R. Keefe[1] | Benjamin Suarez-Jimenez[2] | Xi Zhu[3,4] | Amit Lazarov[3,5] | Ariel Durosky[6] | Sara Such[7] | Caroline Marohasy[8] | Shmuel Lissek[9] | Yuval Neria[2,4,10]

[1]Psychiatry Research Institute at Montefiore Einstein, Albert Einstein College of Medicine, Bronx, New York, USA

[2]Neuroscience Department, University of Rochester, Rochester, New York, USA

[3]Department of Psychiatry, Columbia University Irving Medical Center, New York, New York, USA

[4]New York State Psychiatric Institute, New York, New York, USA

[5]School of Psychological Sciences, Tel-Aviv University, Tel-Aviv, Israel

[6]Department of Psychology, The University of Tulsa, Oklahoma, Tulsa, USA

[7]Department of Psychology, Pennsylvania State University, University Park, Pennsylvania, USA

[8]Department of Psychology, University of Washington, Seattle, Washington, USA

[9]Department of Psychology, University of Minnesota, Minneapolis, Minnesota, USA

[10]Department of Epidemiology, Columbia University Irving Medical Center, New York, New York, USA

Correspondence
Yuval Neria, Department of Psychiatry, Columbia University Irving Medical Center, New York, NY, USA.
Email: ny126@cumc.columbia.edu

Funding information
Brain and Behavior Research Foundation; Israel Science Foundation; National Institute of Mental Health; Clinical & Translational Science Center at Weill Medical College of Cornell University, NIH/NCATS, Grant/Award Number: TL1-TR-002386

Abstract

Background: Patients with posttraumatic stress disorder (PTSD) tend to over-generalize threat to safe stimuli, potentially reflecting aberrant stimuli discrimination. Yet, it is not clear whether threat overgeneralization reflects general discrimination deficits, or rather a specific bias related to aversive stimuli. Here we tested this question and characterized the neural correlates of threat discrimination.

Methods: One-hundred and eight participants (33 PTSD; 43 trauma-exposed controls; 32 healthy controls) completed an emotionally neutral complex shape discrimination task involving identifying in 42 similar pairs the previously observed shape; and an emotionally aversive discrimination task, involving providing risk ratings for an aversive conditioned stimulus (CS+), and for several stimuli gradually differing in size from the original CS+. Resting state functional connectivity (rsFC) was collected before completing the tasks.

Results: No group differences emerged on the emotionally neutral task. Conversely, on the emotionally aversive task, individuals with PTSD had steeper linear risk rating slopes as the stimuli more resembled the conditioned stimulus. Finally, lower rsFC of amygdala-default mode network (DMN) and DMN-salience network (SN) were associated with steeper risk slopes, while for hippocampus-SN, lower rsFC was found only among participants with PTSD.

John R. Keefe, Benjamin Suarez-Jimenez, and Xi Zhu are co-first authors.

Conclusions: Individuals with PTSD show deficits in discrimination only when presented with aversive stimuli. Dysregulated discrimination pattern may relate to a lack of input from regulatory brain areas (e.g., DMN/hippocampus) to threat-related brain areas (e.g., SN/amygdala).

KEYWORDS
fMRI, learning, PTSD, stimuli discrimination, threat

1 | INTRODUCTION

Learning to discriminate between threatening and nonthreatening stimuli in the environment is an important adaptive feature for survival across species (LeDoux, 2014). This discrimination process is typically studied by comparing reactions to an aversively reinforced conditioned stimulus (CS+) to a nonreinforced, neutral, and hence benign stimulus (CS−). Aberrant discrimination processes have long been attributed to fear-related psychopathologies, including, among others, posttraumatic stress disorder (PTSD; Lissek & Grillon, 2012). Specifically, patients with PTSD tend to display fear-related responses towards both the CS+ and CS−, suggesting deficits in stimulus discrimination (Duits et al., 2015; Jovanovic et al., 2012).

Recently, research has more closely examined discrimination deficits via threat overgeneralization—threat-related reactions to stimuli that resemble the original aversive cue, or its ancillary details, when no actual danger exists (Dunsmoor & Paz, 2015; Lissek et al., 2010, 2014; Lopresto et al., 2016; Morey et al., 2020). To study this phenomenon experimentally, several benign stimuli, resembling the CS+ at different degrees, are presented to participants while their reactivity is assessed. The steepness of the emerging gradient (i.e., from the stimulus most resembling the CS+ to the stimulus least resembling it) is then computed and used to estimate levels of threat generalization (Lissek et al., 2008), with steeper gradients representing better discrimination. Indeed, in PTSD, this generalization gradient has been shown to be less steep compared to non-PTSD trauma-exposed counterparts (Kaczkurkin et al., 2017; Thome et al., 2018), reflecting a stronger generalization of the conditioned threat response to safe stimuli resembling the CS+. However, whether this threat overgeneralization reflects a general deficit in discrimination between different stimuli, or rather a more specific aberration related to aversive stimuli only, remains unclear (Bernstein et al., 2020).

Exploring possible brain activation patterns involved in discrimination in general, research has implicated several important brain regions using functional magnetic resonance imaging (fMRI). First, default mode network (DMN)-related brain regions, such as the anterior hippocampal and ventromedial PFC (vmPFC), have been suggested to play a role in pattern separation and discrimination between threat and safety cues (Fullana et al., 2016; Lissek et al., 2014; Marstaller et al., 2017). Second, threat overgeneralization has been specifically attributed to higher activity in the salience network (SN) and dorsomedial prefrontal cortex (dmPFC; Fullana et al., 2016; Kaczkurkin et al., 2017; Morey et al., 2015), with SN regions demonstrating generalization gradients entailing higher activation as stimuli increase in similarity to CS+. Hyperactivation of the SN regions has been proposed to underlie the often-observed persistent and exaggerated threat responses in patients with PTSD, even in the presence of safety cues (Jovanovic et al., 2012; Liberzon & Abelson, 2016). Third, the hippocampus also shows distinct patterns of activation and repetition suppression effects suggestive of pattern separation versus completion by different hippocampal subregions (Dimsdale-Zucker et al., 2018; Schlichting et al., 2015; Yassa & Stark, 2011). Finally, research has also shown that while SN regions demonstrate generalization gradients entailing higher activation as stimuli increase in similarity to CS+, DMN regions and the anterior hippocampus demonstrate the converse pattern (Webler et al., 2021). Taken together, the aforementioned findings suggest that a concert of activity in the hippocampus and vmPFC is needed to effectively encode and retrieve the needed information for discriminating between stimuli, which would then inform the valence of the experience and an appropriate expression of fear through the SN (Webler et al., 2021). Activity differences in these neural circuits have also been noted using resting state MRI comparing PTSD and controls (Koch et al., 2016; Zandvakili et al., 2020; Zilcha-Mano et al., 2020).

While deficits in pattern separation have been hypothesized as a central characteristic of PTSD (Kheirbek et al., 2012), to our knowledge, no study to date has examined the specificity of this deficit—whether it is a general one, pertaining to any differentiation between two patterns, or whether it is specific to situations involving aversive or affectively intense valence. Here, we examined group differences between PTSD and non-PTSD controls (trauma-exposed and nontrauma-exposed) in behavioral discrimination, testing potentially differential responses to an emotionally neutral and an emotionally aversive discrimination task. We also explored the associations between behavioral discrimination performance on each task and resting-state functional connectivity (rsFC) patterns, focusing on brain networks and structures implicated in assigning fear valence to stimuli and fear discrimination processes, as well as possible associations between rsFC patterns and PTSD status (PTSD vs. control groups). Since the emotionally-neutral task was not performed in the scanner, we employed rsFC for this investigation to permit a more comparable examination and differentiation of brain

TABLE 1 Demographic and clinical characteristics of study participants

	HC ($n = 32$)	TEC ($n = 43$)	PTSD ($n = 33$)
Age	35.5 (11.5)	37.4 (11.6)	36.0 (13.6)
Gender (% *M*)	15 (45.5%)	24 (59.8%)	23 (69.7%)
Race			
Caucasian	11 (34.4%)	10 (23.2%)	11 (33.3%)
Black	17 (53.1%)	24 (55.8%)	15 (45.5%)
Asian	0 (0.0%)	4 (9.3%)	2 (6.1%)
NA/PI	3 (9.4%)	5 (11.6%)	4 (12.1%)
Other	1 (3.31%)	1 (2.3%)	1 (3.0%)
Ethnicity (% Hispanic/Latinx)	5 (15.6%)	11 (25.6%)	9 (27.3%)
Years of education	15.2 (3.9)	14.1 (3.2)	13.8 (4.4)
Major depressive disorder (% yes)	0 (0%)	0 (0%)	11 (33.3%)
Persistent depressive disorder (% yes)	0 (0%)	0 (0%)	11 (33.3%)
Anxiety disorder (% yes)	0 (0%)	2 (4.7%)	9 (27.3%)
CAPS	0.0 (0.0)	6.5 (7.7)	35.1 (9.7)
HAM-D	0.4 (0.8)	3.0 (4.2)	13.4 (6.8)
HAM-A	0.2 (0.5)	3.4 (4.9)	15.6 (8.1)

Abbreviations: CAPS, Clinician-Administered PTSD Scale; HAM-A, Hamilton Rating Scale for Anxiety; HAM-D, Hamilton Rating Scale for Depression; HC, Healthy Control; NA/PI, Native American or Pacific Islander; PTSD, posttraumatic stress disorder; TEC, trauma-exposed control.

networks associated with discrimination performance on each task. RsFC may be relevant to task performance as it likely taps into an intrinsic brain network architecture conserved across many types of fMRI tasks (Cole et al., 2014; Elliott et al., 2019), such that rsFC may index individual differences in neurocognition relevant to either task. Moreover, rsFC associated with task performance often has a strong convergence with task associations to task-based fMRI activation or functional connectivity (Cole et al., 2016; Mennes et al., 2010; Zou et al., 2013).

2 | METHODS

2.1 | Participants

One-hundred and eight participants (33 patients with PTSD, 43 TEC, 32 HC; see Table 1 for demographics and clinical characteristics) completed the study protocol. The three groups were matched on age, sex, ethnic origin, and education, stratified by sex. Trauma exposure was defined as experiencing a traumatic event that met the DSM-5 PTSD Criterion A (American Psychiatric Association, 2013). Subjects were recruited by local advertisements, websites, and word-of-mouth referrals and evaluated at the Anxiety Disorders Clinic/New York State Psychiatric Institute. For more information see Supporting Information.

2.2 | Behavioral tasks

2.2.1 | Emotionally neutral discrimination task

Pattern discrimination was assessed with the computer-based Modified Benton Task (Brickman et al., 2014). In each trial (42 trials in total) participants were asked to memorize a Lissajous-figure that was presented on screen for 10 s. A Lissajous-figure is a sinusoidal curve derived in a mathematically controlled manner, with figures differing in the number of horizontal and vertical nodes (see Supporting Information: Figure 1 for stimuli examples). After a delay of 1 s participants were asked to choose the previously presented figure out of two figures of the same Lissajous-order (42 trials; 42 match and 42 foil images). For each participant, the percentage of correct figure matches was calculated.

2.2.2 | Emotionally aversive discrimination task

The threat discrimination task (Kaczkurkin et al., 2017; Lissek et al., 2008) consisted of a string of colored crosshairs presented within a series of circles varying in size. The shock-reinforced CS+ was represented by the biggest or smallest of the circles (counterbalanced across participants). Three additional circles of different sizes, ranging between the smallest and biggest circles, served as the generalization stimuli (GS1, GS2, and GS3 the closest resembling the CS+), which were presented in the absence of shock. If the biggest circle was the CS+, then the smallest served as the unreinforced oCS−, and vice versa. An additional V shaped CS− (vCS−) was included as a noncircular control stimulus (see Supporting Information: Figure 2 for stimuli). Participants were instructed to continuously monitor the stream of colored crosshairs and rate their perceived level of risk for shock as quickly as possible following each red cross. For half of CS/GS trials, one of five crosshairs was red, and the remaining trials included no red crosshairs. Finally, self-reported anxiety to CS+, oCS−, and vCS− were retrospectively assessed following the pre-acquisition, acquisition, and generalization phases using a 10-point scale. The behavioral risk rating indicated valence learning by those who rated the vCS− higher in risk than CS+ during task-related risk rating or the post-task questionnaire (analysis excluded nonlearner participants) leaving 88/110 (80%) of participants with usable behavioral data. Additional details about this task are reported in the Supporting Information. For the purpose of this study, comparing performance on the two emotionally different discriminations tasks (the Modified Benton Task and the threat discrimination task), we collected and analyzed the behavioral data.

2.3 | Data analysis

2.3.1 | Behavioral and clinical data

All nonimaging analyses were conducted within the *R* computing environment (R Core Team, 2021). Linear mixed effects model analyses were conducted using the *R* packages *lme4* (Bates et al., 2015) and *lmerTest* (Kuznetsova et al., 2017). Control covariates in all regressions included age and sex.

2.3.2 | Modified Benton task analyses

Linear regressions were used to predict participants' accuracy (percentage) on the task based on clinical group membership.

2.3.3 | Threat generalization task analyses

Linear mixed effects models were used to predict participants' risk ratings during the Threat Discrimination task based on clinical group membership. Two levels of random effects on risk ratings were specified: a random intercept for each run of the task (early vs. late generalization; Level 2), nested within a random intercept for the participant's overall risk ratings on the task (Level 3). Individual risk ratings (Level 1) were nested within this random effect structure.

Response to each stimulus was assigned a stimulus number reflecting the stimulus' degree of similarity to the original threat CS+ in ascending order, ranging from "0" assigned to the safety stimulus vCS− to the target threat stimulus CS+ labeled a "5." Performance on the task was analyzed through examining the interaction between predictors and the stimulus number, indicating differences in how quickly risk is assigned to a stimulus as a function of its resemblance to the threat stimulus CS+. As such, the basic model included fixed terms of session number (i.e., the linear slope term) and the square of session number (i.e., the quadratic slope term).

2.4 | Resting-state functional connectivity acquisition, data preparation, and analyses

2.4.1 | Acquisition and data preparation

One hundred and eight participants were scanned using either a 3T General Electric MR750 ($n = 74$) or a 3T General Electric PREMIER ($n = 36$; GE Medical Systems) equipped with a 32-channel receive-only head coil was used. For each participant a high-resolution T1-weighted 3D BRAVO sequence was acquired using the following parameter: T1 = 450 mm, Flip angle = 12°, field of view = 25.6 cm, 256 × 256 matrix, slice thickness = 1 mm. T2*-weighted echo-planar images (EPIs) depicting the blood-oxygen-level-dependent (BOLD) were acquired for each participant with TR = 1.3 s, TE = 28 msec, FA = 60°, FOV = 19.2 cm, number of slices = 27, slice thickness = 4 mm. For each participant, 6 min of resting state scanning was acquired. A head cushion was used to limit head motion.

All resting state MRI images were preprocessed using MATLAB version R2020a (The MathWorks, Inc.) and statistical parametric mapping software (SPM12; Welcome Trust Centre for Neuroimaging, UCL). Preprocessing steps can be found in the Supporting Information.

2.4.2 | Neuroimaging analyses

region of interest (ROI)-to-ROI connectivity analysis was performed using CONN Functional Connectivity toolbox v13 (Whitfield-Gabrieli & Nieto-Castanon, 2012). Band-pass filtering with a frequency window of 0.01 to 0.09 Hz was performed. All ROIs were defined based on CONN's ICA analyses of the HCP data set of 497 participants. The mean BOLD time series was computed across all voxels within each ROI. Bivariate-regression analyses were used to determine the linear association of the BOLD time series between each seed ROI and all other target ROI for each participant. The resultant correlation coefficients were transformed into *z*-scores using Fisher's transformation to satisfy normality assumptions.

ROI-to-ROI connectivity analysis was performed using ROIs identified as key nodes in three networks of interest: (a) a Central Executive Network (CEN) component consisting of the left and right lateral prefrontal cortex and left and right posterior parietal; (b) a Default Mode Network (DMN) component consisting of the ventromedial prefrontal cortex, posterior cingulate cortex, and the left and right angular gyrus; and (c) a Salience Network (SN) component consisting of dorsal anterior cingulate cortex, left and right anterior insula, left and right rostral prefrontal cortex, and left and right supramarginal gyrus. Average within- and between- network connectivity of these three networks and each other network was calculated. We also separately included amygdala and hippocampus as ROIs (defined by Harvard-Oxford subcortical Atlas) involved in pattern completion/separation, threat, and emotional memories (Janak & Tye, 2015; Lisman et al., 2017), and furthermore calculated the average connectivity between these regions and the above three networks.

For our analyses concerning the relationships between the rsFC and emotionally aversive versus emotionally neutral discrimination tasks performance, we employed the Benjamini-Hochberg correction for the false discovery rate (Benjamini & Hochberg, 1995) within each regression. These *p* values are reported as "adjusted" *p* values throughout. Control covariates in all regressions included age, sex, and scanner site to control for possible between-scanner differences. For statistically significant relations, we also report between-scanner findings separately in the Supporting Information.

2.4.3 | Association between the modified Benton task and rsFC analyses

Linear regressions were used to predict participants' accuracy (percentage) on the task based on clinical group membership and

functional connectivity indices. We examined the relationships of within- and between- network connectivity and performance on the Modified Benton task, wherein between- and within-connectivity were analyzed within two separate linear regression models.

2.4.4 | Association between the threat generalization task and rsFC analyses

Linear mixed effects models were used as described above to predict participants' risk ratings related to rsFC during the Threat Discrimination task based on clinical group membership and functional connectivity indices. The basic model included fixed terms of session number (i.e., the linear slope term) and the square of session number (i.e., the quadratic slope term). Significant interactions between either slope term or a predictor (e.g., rsFC value) indicated that participants exhibited differences in how their risk ratings changed as a stimulus more resembled the threat CS+ stimulus, as a function of a given predictor. We examined both the relationships of within- and between- network connectivity and performance on the Threat Discrimination task, wherein between- and within-connectivity were analyzed within two separate linear mixed models. No within-network results were statistically significant, and these results are reported in the Supporting Information.

2.4.5 | Predicting PTSD status

Presence of PTSD was predicted using a logistic regression, wherein being diagnosed with PTSD was coded as a "1." Within- and between-network rsFC were examined in separate logistic regressions as predictors.

3 | RESULTS

3.1 | Task performance and clinical status

3.1.1 | Emotionally neutral discrimination task (modified Benton task)

Participants with PTSD did not differ in their performance on the Modified Benton accuracy from the participants without PTSD ($B = 0.01$ [95% CI: −0.04 to 0.05], $t[105] = 0.36$, $p = .719$, $d = 0.10$; see Figure 1; see Supplemental Information: Figure 4 for score distribution). There were no significant pairwise differences between the individual groups (PTSD; HC; TEC; $F[3,103] = 0.31$, $p = .817$).

3.1.2 | Emotionally aversive discrimination task (threat generalization task)

We examined differences between participants with and without PTSD in terms of their linear slope of risk ratings (i.e., to what extent do they make higher risk ratings as stimuli more resemble the threat CS+) *and* their quadratic slopes, which reflects the extent to which the slopes of risk ratings become more or less steep (or accelerate/decelerate) as stimuli more resembled the threat CS+.

Participants with PTSD exhibited significantly different slopes of change in risk compared to participants without PTSD (see Figure 2). PTSD status significantly interacted with both the linear ($B = 0.22$ [95% CI: 0.09, 0.34], $t[760] = 3.40$, $p < .001$) and quadratic stimulus number terms ($B = -0.04$ [95% CI: −0.06, −0.01], $t[760] = -2.93$, $p = .004$), such that participants with PTSD had a stronger linear slope component and a weaker quadratic component. Overall, compared to controls, patients with PTSD displayed more linear increases in risk ratings as the stimulus increased in resemblance to the CS+. Moreover, while participants without PTSD showed steeper increases in risk ratings only as the stimulus increased in resemblance to the CS+ (i.e., they only began to make higher risk ratings for the more similar vs. less similar stimuli), participants with PTSD showed more linear slopes.[‡]

There were also significant pairwise differences in slopes of risk ratings between groups ($F[3,760] = 4.48$, $p = .004$ linear; $F[3,760] = 3.54$, $p = .015$ quadratic). Specifically, PTSD participants differed from trauma-exposed healthy controls ($B = 0.18$ [95% CI: 0.04, 0.33], $t[760] = 2.47$, $p = .014$ linear; $B = -0.03$ [95% CI: −0.00, −0.06], $t[760] = 2.16$, $p = .031$ quadratic) and healthy controls ($B = 0.28$ [95% CI: 0.13, 0.43], $t[760]=3.54$, $p < .001$ linear; $B = -0.05$ [95% CI: −0.08, −0.02], $t[760] = -3.15$, $p = .003$ quadratic), showing stronger linear and weaker quadratic slope components (see Supporting Information: Figure 3 for PTSD compared to other groups).

3.2 | Resting-state functional connectivity

3.2.1 | Emotionally neutral discrimination task (modified Benton task)

Echoing the behavioral results described above, no rsFC patterns between included networks/regions significantly predicted accuracy on the Modified Benton task (see Table 2).

3.2.2 | Emotionally aversive discrimination task (threat generalization task)

After correction for multiple comparisons, three between-networks rsFC pathways predicted the steepness of linear slopes of risk ratings (see Supporting Information: Figure 5). Lower rsFC amygdala-DMN ($B = -0.17$ [95 CI: −0.27, −0.07], $t[759] = -3.36$, $p < .001$, adjusted

[‡]In a supplemental analysis (see Supporting Information), we also examined which risk ratings for individual stimuli differed significantly between participants with versus without PTSD, and which generalization stimuli (GS1, 2, 3) were significantly different from the conditioned ring-shaped safety stimulus (oCS−).

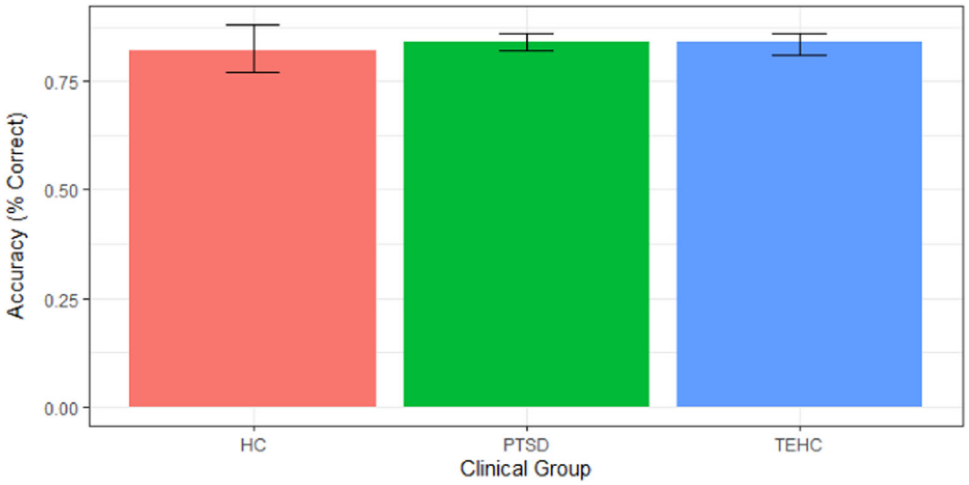

FIGURE 1 Percentage correct figure matches on the emotionally neutral discrimination/Modified Benton task per group. HC, healthy control; PTSD, posttraumatic stress disorder; TEHC, trauma-exposed health control. Bars represent 95% confidence intervals for mean performance within group. Participants did not differ on performance (% correct vs. incorrect matches) on the emotionally neutral discrimination task as a function of their clinical group ($F[3,103] = 0.31$, $p = .817$).

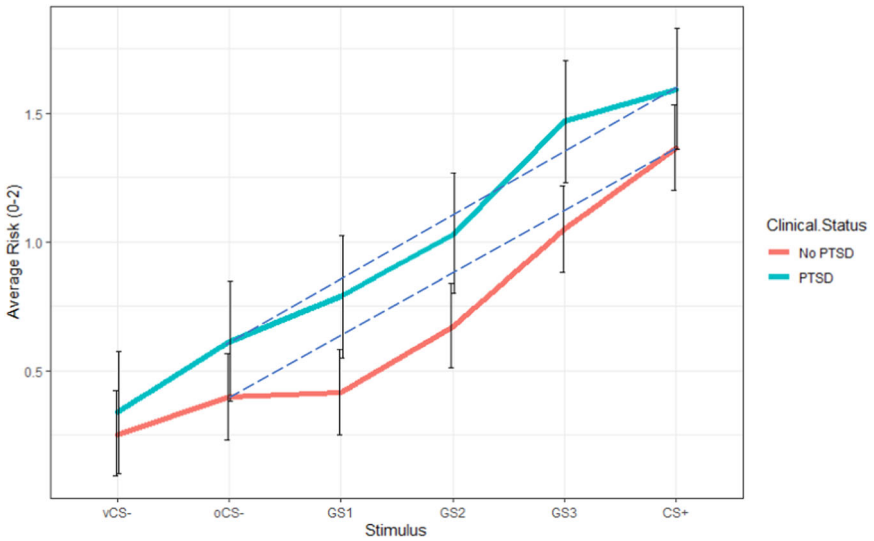

FIGURE 2 Emotionally aversive discrimination task performance as a function of PTSD status. vCS−, V-shaped conditioned safety signal; oCS−, ring-shaped conditioned safety signal; GS1-3, generalization stimuli, higher numbers more resemble CS+, CS+, aversive conditioned stimulus. Bars are 95% confidence intervals for between-group estimates of risk ratings for a given stimulus. Dotted lines illustrate deviations from a linear slope. Patients with PTSD exhibited significantly different linear ($p < .001$) and quadratic ($p = .004$) slopes of change in risk rating as stimuli more closely resembled the conditioned aversive stimulus compared to other participants. On an individual level, stimuli GS1 ($p = .012$), GS2 ($p = .015$), and GS3 ($p = .005$) were given significantly greater risk scores by patients with PTSD relative to other participants.

$p = .005$), DMN-SN ($B = -0.23$ [95% CI: −0.37, −0.09], $t[757] = -3.24$, $p = .001$, adjusted $p = .005$), and hippocampus-SN ($B = -0.19$ [−0.32, −0.06], $t[759] = -2.79$, $p = .005$, adjusted $p = .017$) predicted steeper linear increases in risk ratings as the stimulus increased in resemblance to the CS+ (see Table 3 for all pathways). None of the pathways that significantly related to linear slopes of risk ratings also interacted significantly with the quadratic slope term (*p*s > .5).

For rsFC pathways significantly predicting risk rating slopes, we examined whether PTSD status moderated the relationship between these pathways. The relationship between the hippocampus-SN pathway and linear risk rating slopes was significantly moderated by presence of PTSD ($B = -0.32$ [95% CI: −0.59, −0.05], $t[755] = -2.33$, $p = .020$; see Figure 3). Among participants without PTSD, there was no relationship between hippocampus-SN rsFC and linear risk rating slopes ($B = -0.05$ [95% CI: −0.19, 0.08], $t[755] = -0.75$, $p = .457$). By contrast, among participants with PTSD, a higher hippocampus-SN rsFC was related to a relatively less steep risk slope ($B = -0.37$ [95% CI: −0.61, −0.14], $t[755] = -3.13$, $p = .002$). However, there was no moderation by PTSD status of either the amygdala-DMN ($B = -0.00$ [95% CI: −0.22, 0.22], $t[754] = -0.02$, $p = .983$) or DMN-SN

relationships ($B = 0.27$ [95% CI: −0.10, 0.63], $t[755] = 1.43$, $p = .154$) to linear risk rating slopes.

3.2.3 | Clinical status

Several between-network connectivity patterns were potentially related to PTSD status. In particular, higher rsFC amygdala-DMN (log odds = −6.56 [95%CI: −12.07, −1.05], $Z = -2.33$, $p = .020$, adjusted $p = .090$) and hippocampus-SN rsFC (log odds = −7.74 [95% CI: −13.91, −1.56], $Z = -2.46$, $p = .014$, adjusted $p = .090$) predicted less frequency of PTSD status, while higher amygdala-SN rsFC predicted greater frequency of PTSD status (log odds = 5.51 [95% CI: 0.16, 10.86], $Z = 2.02$, $p = .043$, adjusted $p = .129$; see Table 4 for all results). However, these results were not significant after statistical correction for multiple comparisons.

TABLE 2 Accuracy on the Modified Benton task as predicted by between-networks/region functional connectivity

Connectivity path	Semipartial *r* with accuracy	*p* Value	Adjusted *p* Value
Amygdala-CEN	−0.15	.137	.457
Amygdala-DMN	0.16	.104	.457
Amygdala-hippocampus	0.10	.288	.576
Amygdala-SN	−0.06	.529	.688
CEN-DMN	0.02	.822	.822
CEN-hippocampus	0.11	.244	.576
CEN-SN	−0.06	.529	.688
DMN-hippocampus	−0.19	.050	.457
DMN-SN	−0.06	.550	.688
Hippocampus-SN	−0.03	.739	.821

Note: Relationships between functional connectivity pathways and Modified Benton task accuracy was examined in a linear regression including all listed pathways, controlling for age, gender, and scanner site. Semipartial correlations are reported. Adjusted *p* Values reflect a Benjamini-Hochberg correction for the false discovery rate.

Abbreviations: CEN, central executive network; DMN, default mode network; SN, salience network.

4 | DISCUSSION

In the present study, participants with and without PTSD (trauma-exposed and healthy controls) completed an emotionally neutral complex shape discrimination task, as well as an emotionally aversive discrimination task. Findings showed that patients with PTSD performed as well as trauma-exposed and healthy controls on the emotionally neutral discrimination task, but exhibited discrimination deficits on the emotionally aversive discrimination task. Echoing these behavioral results, rsFC patterns did not predict emotionally neutral discrimination task performance, but were predictive of performance on the emotionally aversive discrimination task. Specifically, behavioral results on this task were associated with lower amygdala-DMN, DMN-SN, and hippocampus-SN rsFC, which further predicted both steeper linear slopes of risk ratings on the task and, at a trend level following statistical correction, having a PTSD diagnosis.

Our findings suggest that difficulties discriminating between similar visual stimuli only manifest among patients with PTSD when faced with affectively threatening situations. If deficits in more basic visual discrimination functions were responsible for overgeneralized threat responding among PTSD patients, it is likely that behavioral differences between groups would have

TABLE 3 Slopes of change in risk rating (stimulus number 0–5) as predicted by between-networks/region functional connectivity

Connectivity path	*B* linear slope [95% CI]	Standardized beta	*p* Value	Adjusted *p* Value
Amygdala-CEN	−0.01 [−0.13, 0.10]	−.01	.803	.870
Amygdala-DMN	−0.17 [−0.27, −0.07]	−.06	<.001	.005
Amygdala-hippocampus	0.01 [−0.07, 0.08]	.00	.862	.870
Amygdala-SN	0.01 [−0.10, 0.13]	.01	.815	.870
CEN-DMN	−0.01 [−0.11, 0.10]	−.00	.870	.870
CEN-hippocampus	−0.05 [−0.17, 0.07]	−.02	.428	.713
CEN-SN	−0.07 [−0.21, 0.06]	−.02	.295	.593
DMN-hippocampus	−0.10 [−0.19, −0.01]	−.04	.028	.070
DMN-SN	−0.23 [−0.37, −0.09]	−.07	.001	.005
Hippocampus-SN	−0.19 [−0.32, −0.06]	−.06	.005	.017

Note: Slopes were analyzed in a linear mixed model including all listed pathways, controlling for age, gender, and scanner site. Adjusted *p* Values reflect a Benjamini-Hochberg correction for the false discovery rate.

Abbreviations: CEN, central executive network; DMN, default mode network.

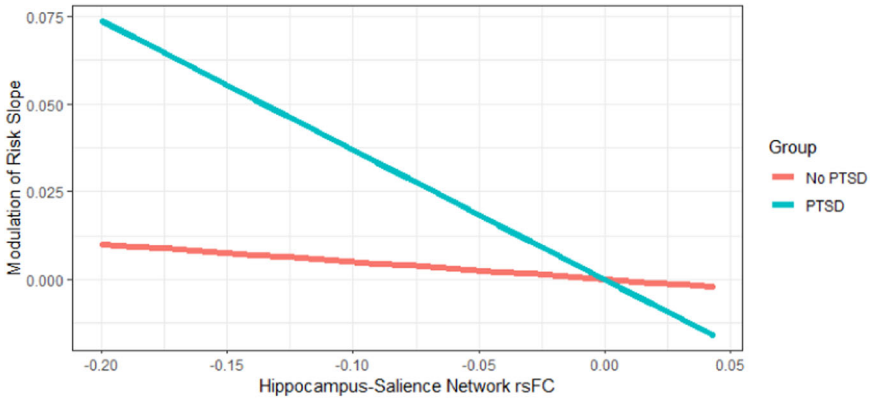

FIGURE 3 Moderation of the relationship between Hippocampus-Salience Network resting-state functional connectivity and linear risk rating slopes on the emotional discrimination task. rsFC, resting-state functional connectivity. The relationship between the hippocampus-SN pathway and linear risk rating slopes was significantly moderated by presence of PTSD ($p = .020$). Among participants without PTSD, there was no relationship between hippocampus-SN rsFC and linear risk rating slopes ($p = .457$). By contrast, among participants with PTSD, a higher (i.e., more positive) hippocampus-SN rsFC was related to a relatively less steep risk slope ($p = .002$).

TABLE 4 Association between PTSD status and between-networks/region functional connectivity

Connectivity path	Log odds [95% CI]	*p* Value	Adjusted *p* Value
Amygdala-CEN	2.96 [−1.46, 7.39]	.189	.425
Amygdala-DMN	−6.56 [−12.07, −1.05]	.020	.090
Amygdala-hippocampus	0.99 [−1.69, 3.66]	.469	.704
Amygdala-SN	5.51 [0.16, 10.86]	.043	.129
CEN-DMN	−0.81 [−5.57, 3.94]	.737	.807
CEN-hippocampus	0.78 [−3.97, 5.53]	.748	.807
CEN-SN	−0.70 [−6.36, 4.95]	.807	.807
DMN-hippocampus	−1.99 [−6.52, 2.54]	.390	.702
DMN-SN	−0.95 [−7.05, 5.14]	.759	.807
Hippocampus-SN	−7.34 [−13.91, −1.56]	.014	.090

Note: Relationships between functional connectivity pathways and PTSD status were examined in a logistic regression including all listed pathways, controlling for age, sex, and scanner site. Adjusted *p* Values reflect a Benjamini-Hochberg correction for the false discovery rate.

Abbreviations: CEN, central executive network; DMN, default mode network.

also emerged on the emotionally neutral task. By contrast, and in line with previous studies (Kaczkurkin et al., 2017; Webler et al., 2021), we observed overgeneralized threat responding on the emotionally aversive task among participants with PTSD. While performance on this task also requires visual discrimination, here one needs to also learn which stimuli were associated with a shock. Following the present study, which directly compared nonemotion and emotionally aversive discrimination in PTSD, future research can reveal more fine-grained mechanisms by which patients with PTSD experience overgeneralized threat by directly comparing emotionally aversive discrimination with other emotionally relevant discrimination contexts, such as reward learning, which may be disrupted in PTSD, either generally, or particularly when avoiding trauma cues (Seidemann et al., 2021; Weaver et al., 2020).

Our rsFC-based findings of the emotionally aversive discrimination task demonstrated that lower (i.e., more negative/anticorrelated) amygdala-DMN, DMN-SN, and hippocampus-SN rsFC each predicted higher risk ratings as stimuli increased in resemblance to the CS+, mirroring the behavioral findings of patients with PTSD. Lesion studies in mammals suggest that the hippocampus is obligate for most forms of fear conditioning to context (e.g., Antoniadis & McDonald, 2000), and in humans both general mnemonic and fear generalization tasks performed in-scanner suggest that the hippocampus is critical for pattern separation allowing for accurate discrimination between stimuli (Nash et al., 2021; Webler et al., 2021). Higher rsFC between the hippocampus-SN may reflect heightened discrimination supported by the hippocampus (Rolls, 2013; Yassa & Stark, 2011), functioning to moderate the degree to which a similar, but non-CS+, stimulus is evaluated as a threat by SN regions. In

addition, patients with PTSD (but not controls), who generally had diminished hippocampus-SN connectivity, were able to exhibit more accurate emotionally aversive discrimination inasmuch as they exhibited relatively stronger hippocampus-SN connectivity. This pattern provides further evidence for a mechanism by which hippocampus-mediated discrimination modulates the SN that may be overly active or sensitized among patients with PTSD (Zilcha-Mano et al., 2020).

On the other hand, positive amygdala-DMN and DMN-SN rsFC may promote more accurate performance in emotionally aversive discrimination via the DMN's involvement in employing personal/environmental context (e.g., memories of the conditioning) to construct discrete emotional experiences, incorporating affective signals (e.g., fear) from the amygdala and SN (Satpute & Lindquist, 2019). DMN activation is generally anticorrelated with networks associated with fear processing, and it also increases with safety learning (Marstaller et al., 2017; Webler et al., 2021), suggesting that the DMN may be involved in generating safety signals through contextualization, limiting overgeneralization of fear. Our findings are consistent with a perspective that the DMN may regulate amygdala/SN activity subserving fear generalization (Marstaller et al., 2017). Alternatively, this may reflect modulation of amygdala-based fear by the vmPFC (a DMN component). Overall, a reduced amygdala-DMN and DMN-SN rsFC, in concert with reduced hippocampus-SN rsFC, among patients with PTSD implicates an emotionally aversive discrimination system biased toward bottom-up, overly sensitive, and relatively nonspecific processing. This processing deficit is less modulated by neural systems serving to refine pattern detection, such as top-down regulation from the DMN and core discrimination functions of the hippocampus.

Our results suggest that similar rsFC patterns, characterizing diminished performance on the emotionally aversive discrimination task, may also predict PTSD. Results revealed that compared with controls, at a trend level following statistical correction for multiple comparisons, patients with PTSD showed lower amygdala-DMN and hippocampus-SN connectivity. These findings are in accordance with a growing body of research identifying DMN and SN rsFC as distinguishing patients with PTSD from both trauma-exposed and unexposed healthy controls (Koch et al., 2016; Zandvakili et al., 2020; Zilcha-Mano et al., 2020). Heightened amygdala-SN rsFC observed in patients with PTSD may be due to diminished input from top-down regulatory inputs from the prefrontal cortex (e.g., the vmPFC, part of the amygdala-DMN pathway), or from the hippocampus. The rsFC differences between patients with PTSD and controls may reflect neurobiological signatures of PTSD following exposure to trauma (e.g., sensitization of the SN), or a premorbid vulnerability (e.g., emotionally aversive discrimination deficits) influencing likelihood of developing PTSD after trauma. Considering from a therapeutic standpoint, PTSD interventions encouraging discrimination/separation may be reflected in relative increases in intrinsic rsFC of the above-noted pathways. Examining the covariance and temporality of changes in PTSD symptoms, emotionally aversive discrimination performance, and network rsFC in clinical trials may further elucidate the mechanisms of successful PTSD treatments, and perhaps pinpoint which patients may benefit from specific interventions modulating these neural networks (Neria, 2021).

Several limitations are worth noting. First, accuracy on the emotionally neutral discrimination task was relatively high (mean 83.8%) potentially reflecting a ceiling effect (see Supporting Information: Figure 4 for histogram). Employing a more difficult task might have revealed a different pattern of findings. Second, due to concerns for participant burden and discomfort we could only do the emotionally aversive task within the scanner. Therefore, the two tasks were performed in different settings (emotionally aversive task in-scanner vs. emotionally neutral task out-of-scanner), which may have affected the comparability of performance across the two tasks. We did not think it would be interpretable to employ activation maps generated by one task (emotionally aversive) but not the other (emotionally neutral). However, the rsFC networks associated with task performance on the emotionally aversive task converge with those activated during fMRI task performance in fear learning and discrimination paradigms reported in the literature (summarized in Webler et al., 2021). Third, for both the amygdala and hippocampus, our ROIs encompassed the whole structure and did not distinguish between subregions, while both animal and human work has suggested differential roles for subregions in mediating fear/anxiety and memory (Adhikari et al., 2015; Duncan & Schlichting, 2018; Jimenez et al., 2018; Lazarov et al., 2017). However, our hippocampus-SN analysis showed no subregion-specific pathway driven by anterior or posterior hippocampus (see Supporting Information), which have been found to have clinically important differences in PTSD (Lazarov et al., 2017; Suarez-Jimenez et al., 2020). This could primarily be due to the relatively small sample of this study, which lowered the study's power to find group differences in such small areas. Larger samples could examine more fine-grained amygdala/hippocampus ROIs—or regions of the DMN/SN—to understand more precisely the neural mechanisms involved in PTSD and its impacts on emotionally aversive discrimination.

In conclusion, the present study demonstrates that deficits in emotionally aversive—but not emotionally neutral—discrimination may be specific to threat in PTSD. Heightened connectivity between brain networks supporting ascribing threat to stimuli, and discriminating between similar stimuli, may protect against over-response and attribution of danger to CS−, and thus potentially PTSD.

ACKNOWLEDGMENTS

This research was supported by NIMH grant R01MH105355-01A1 (Dr Neria). Dr. Suarez-Jimenez was supported by K01MH118428 and Brain & Behavior Research Foundation. Dr. Zhu was supported by K01MH122774 and Brain & Behavior Research Foundation. Dr. Lazarov was supported by Israel Science Foundation grant 374/20. Dr. John Keefe was supported by NIH/NCATS Grant # TL1-TR-002386 through the Clinical & Translational Science Center at Weill Medical College of Cornell University.

CONFLICT OF INTEREST

The authors declare no conflict of interest.

DATA AVAILABILITY STATEMENT

The data that support the findings of this study are available from the corresponding author upon reasonable request.

ETHICS STATEMENT

This study was approved by the New York State Psychiatric Institute—Columbia University Department of Psychiatry IRB, protocol #: 7136, protocol name "Neural Signature of Trauma." All participants received informed consent for participation in the study and signed an informed consent form.

REFERENCES

Adhikari, A., Lerner, T. N., Finkelstein, J., Pak, S., Jennings, J. H., Davidson, T. J., Ferenczi, E., Gunaydin, L. A., Mirzabekov, J. J., Ye, L., Kim, S. -Y., Lei, A., & Deisseroth, K. (2015). Basomedial amygdala mediates top-down control of anxiety and fear. *Nature*, *527*(7577), 179–185. https://doi.org/10.1038/nature15698

American Psychiatric Association. (2013). *Diagnostic and statistical manual of mental disorders* (5th ed.). American Psychiatric Association. https://doi.org/10.1176/appi.books.9780890425596

Antoniadis, E. (2000). Amygdala, hippocampus and discriminative fear conditioning to context. *Behavioural Brain Research*, *108*(1), 1–19. https://doi.org/10.1016/s0166-4328(99)00121-7

Bates, D., Mächler, M., Bolker, B., & Walker, S. (2015). Fitting linear mixed-effects models using lme4 [sparse matrix methods; linear mixed models; penalized least squares; Cholesky decomposition]. *Journal of Statistical Software*, *67*, 1–48. https://doi.org/10.18637/jss.v067.i01

Benjamini, Y., & Hochberg, Y. (1995). Controlling the false discovery rate: A practical and powerful approach to multiple testing. *Journal of the Royal Statistical Society: Series B (Methodological)*, *57*(1), 289–300. http://www.jstor.org/stable/2346101

Bernstein, E. E., Brühl, A., Kley, H., Heinrichs, N., & McNally, R. J. (2020). Mnemonic discrimination in treatment-seeking adults with and without PTSD. *Behaviour Research and Therapy*, *131*, 103650. https://doi.org/10.1016/j.brat.2020.103650

Brickman, A. M., Khan, U. A., Provenzano, F. A., Yeung, L. -K., Suzuki, W., Schroeter, H., Wall, M., Sloan, R. P., & Small, S. A. (2014). Enhancing dentate gyrus function with dietary flavanols improves cognition in older adults. *Nature Neuroscience*, *17*(12), 1798–1803. https://doi.org/10.1038/nn.3850

Cole, M. W., Bassett, D. S., Power, J. D., Braver, T. S., & Petersen, S. E. (2014). Intrinsic and task-evoked network architectures of the human brain. *Neuron*, *83*(1), 238–251. https://doi.org/10.1016/j.neuron.2014.05.014

Cole, M. W., Ito, T., Bassett, D. S., & Schultz, D. H. (2016). Activity flow over resting-state networks shapes cognitive task activations. *Nature Neuroscience*, *19*(12), 1718–1726. https://doi.org/10.1038/nn.4406.

Core Team, R. (2021). *R: A language and environment for statistical computing. In (Version 4.0.4) R Foundation for Statistical Computing*. https://www.R-project.org/

Dimsdale-Zucker, H. R., Ritchey, M., Ekstrom, A. D., Yonelinas, A. P., & Ranganath, C. (2018). CA1 and CA3 differentially support spontaneous retrieval of episodic contexts within human hippocampal subfields. *Nature Communications*, *9*(1), 294. https://doi.org/10.1038/s41467-017-02752-1

Duits, P., Cath, D. C., Lissek, S., Hox, J. J., Hamm, A. O., Engelhard, I. M., van den Hout, M. A., & Baas, J. M. P. (2015). Updated meta-analysis of classical fear conditioning in the anxiety disorders. *Depression and Anxiety*, *32*(4), 239–253. https://doi.org/10.1002/da.22353

Duncan, K. D., & Schlichting, M. L. (2018). Hippocampal representations as a function of time, subregion, and brain state. *Neurobiology of Learning and Memory*, *153*, 40–56. https://doi.org/10.1016/j.nlm.2018.03.006

Dunsmoor, J. E., & Paz, R. (2015). Fear generalization and anxiety: Behavioral and neural mechanisms. *Biological Psychiatry*, *78*(5), 336–343. https://doi.org/10.1016/j.biopsych.2015.04.010

Elliott, M. L., Knodt, A. R., Cooke, M., Kim, M. J., Melzer, T. R., Keenan, R., Ireland, D., Ramrakha, S., Ramrakha, S., Poulton, R., Caspi, A., Moffitt, T. E., & Hariri, A. R. (2019). General functional connectivity: Shared features of resting-state and task fMRI drive reliable and heritable individual differences in functional brain networks. *NeuroImage*, *189*, 516–532. https://doi.org/10.1016/j.neuroimage.2019.01.068

Fullana, M. A., Harrison, B. J., Soriano-Mas, C., Vervliet, B., Cardoner, N., Àvila-Parcet, A., & Radua, J. (2016). Neural signatures of human fear conditioning: An updated and extended meta-analysis of fMRI studies. *Molecular Psychiatry*, *21*(4), 500–508. https://doi.org/10.1038/mp.2015.88

Janak, P. H., & Tye, K. M. (2015). From circuits to behaviour in the amygdala. *Nature*, *517*(7534), 284–292. https://doi.org/10.1038/nature14188

Jimenez, J. C., Su, K., Goldberg, A. R., Luna, V. M., Biane, J. S., Ordek, G., Zhou, P., Ong, S. K., Wright, M. A., Zweifel, L., Paninski, L., Hen, R., & Kheirbek, M. A. (2018). Anxiety cells in a hippocampal-hypothalamic circuit. *Neuron*, *97*(3), 670–683. https://doi.org/10.1016/j.neuron.2018.01.016

Jovanovic, T., Kazama, A., Bachevalier, J., & Davis, M. (2012). Impaired safety signal learning may be a biomarker of PTSD. *Neuropharmacology*, *62*(2), 695–704. https://doi.org/10.1016/j.neuropharm.2011.02.023

Kaczkurkin, A. N., Burton, P. C., Chazin, S. M., Manbeck, A. B., Espensen-Sturges, T., Cooper, S. E., Sponheim, S. R., & Lissek, S. (2017). Neural substrates of overgeneralized conditioned fear in PTSD. *American Journal of Psychiatry*, *174*(2), 125–134. https://doi.org/10.1176/appi.ajp.2016.15121549

Kheirbek, M. A., Klemenhagen, K. C., Sahay, A., & Hen, R. (2012). Neurogenesis and generalization: A new approach to stratify and treat anxiety disorders. *Nature Neuroscience*, *15*(12), 1613–1620. https://doi.org/10.1038/nn.3262

Koch, S. B. J., van Zuiden, M., Nawijn, L., Frijling, J. L., Veltman, D. J., & Olff, M. (2016). Aberrant resting-state brain activity in posttraumatic stress disorder: A meta-analysis and systematic review. *Depression and Anxiety*, *33*(7), 592–605.

Kuznetsova, A., Brockhoff, P. B., & Christensen, R. H. B. (2017). lmerTest package: Tests in linear mixed effects models [denominator degree of freedom, Satterthwaite's approximation, ANOVA, R, linear mixed effects models, lme4]. *Journal of Statistical Software*, *82*(13), 26. https://doi.org/10.18637/jss.v082.i13

Lazarov, A., Zhu, X., Suarez-Jimenez, B., Rutherford, B. R., & Neria, Y. (2017). Resting-state functional connectivity of anterior and posterior hippocampus in posttraumatic stress disorder. *Journal of Psychiatric Research*, *94*, 15–22. https://doi.org/10.1016/j.jpsychires.2017.06.003

LeDoux, J. E. (2014). Coming to terms with fear. *Proceedings of the National Academy of Sciences*, *111*(8), 2871–2878. https://doi.org/10.1073/pnas.1400335111

Liberzon, I., & Abelson, J. L. (2016). Context processing and the neurobiology of post-traumatic stress disorder. *Neuron*, *92*(1), 14–30. https://doi.org/10.1016/j.neuron.2016.09.039

Lisman, J., Buzsáki, G., Eichenbaum, H., Nadel, L., Ranganath, C., & Redish, A. D. (2017). Viewpoints: How the hippocampus contributes to memory, navigation and cognition. *Nature Neuroscience*, *20*(11), 1434–1447. https://doi.org/10.1038/nn.4661

Lissek, S., Biggs, A. L., Rabin, S. J., Cornwell, B. R., Alvarez, R. P., Pine, D. S., & Grillon, C. (2008). Generalization of conditioned fear-potentiated startle in humans: Experimental validation and clinical relevance. *Behaviour Research and Therapy*, *46*(5), 678–687. https://doi.org/10.1016/j.brat.2008.02.005

Lissek, S., Bradford, D. E., Alvarez, R. P., Burton, P., Espensen-Sturges, T., Reynolds, R. C., & Grillon, C. (2014). Neural substrates of classically conditioned fear-generalization in humans: A parametric fMRI study. *Social Cognitive and Affective Neuroscience*, *9*(8), 1134–1142. https://doi.org/10.1093/scan/nst096

Lissek, S., & Grillon, C. (2012). Learning models of PTSD. In J. G.Beck, & D. M. Sloan (Eds.), (Eds.),*The Oxford handbook of traumatic stress disorders* (pp. 175–190). Oxford University Press. https://doi.org/10.1093/oxfordhb/9780195399066.013.0013

Lissek, S., Kaczkurkin, A. N., Rabin, S., Geraci, M., Pine, D. S., & Grillon, C. (2014). Generalized anxiety disorder is associated with overgeneralization of classically conditioned fear. *Biological Psychiatry*, *75*(11), 909–915. https://doi.org/10.1016/j.biopsych.2013.07.025

Lissek, S., Rabin, S., Heller, R. E., Lukenbaugh, D., Geraci, M., Pine, D. S., & Grillon, C. (2010). Overgeneralization of conditioned fear as a pathogenic marker of panic disorder. *American Journal of Psychiatry*, *167*(1), 47–55. https://doi.org/10.1176/appi.ajp.2009.09030410

Lopresto, D., Schipper, P., & Homberg, J. R. (2016). Neural circuits and mechanisms involved in fear generalization: Implications for the pathophysiology and treatment of posttraumatic stress disorder. *Neuroscience and Biobehavioral Reviews*, *60*, 31–42. https://doi.org/10.1016/j.neubiorev.2015.10.009

Marstaller, L., Burianová, H., & Reutens, D. C. (2017). Adaptive contextualization: A new role for the default mode network in affective learning. *Human Brain Mapping*, *38*(2), 1082–1091. https://doi.org/10.1002/hbm.23442

Mennes, M., Kelly, C., Zuo, X. -N., Di Martino, A., Biswal, B. B., Castellanos, F. X., & Milham, M. P. (2010). Inter-individual differences in resting-state functional connectivity predict task-induced BOLD activity. *NeuroImage*, *50*(4), 1690–1701. https://doi.org/10.1016/j.neuroimage.2010.01.002

Morey, R. A., Dunsmoor, J. E., Haswell, C. C., Brown, V. M., Vora, A., Weiner, J., Stjepanovic, D., Wagner, H. R., & LaBar, K. S. (2015). Fear learning circuitry is biased toward generalization of fear associations in posttraumatic stress disorder. *Translational Psychiatry*, *5*(12):e700. https://doi.org/10.1038/tp.2015.196

Morey, R. A., Haswell, C. C., Stjepanović, D., Dunsmoor, J. E., & LaBar, K. S. (2020). Neural correlates of conceptual-level fear generalization in posttraumatic stress disorder. *Neuropsychopharmacology*, *45*(8), 1380–1389. https://doi.org/10.1038/s41386-020-0661-8

Nash, M. I., Hodges, C. B., Muncy, N. M., & Kirwan, C. B. (2021). Pattern separation beyond the hippocampus: A high-resolution whole-brain investigation of mnemonic discrimination in healthy adults. *Hippocampus*, *31*(4), 408–421. https://doi.org/10.1002/hipo.23299

Neria, Y. (2021). Functional neuroimaging in PTSD: From discovery of underlying mechanisms to addressing diagnostic heterogeneity. *American Journal of Psychiatry*, *178*(2), 128–135. https://doi.org/10.1176/appi.ajp.2020.20121727

Rolls, E. (2013). The mechanisms for pattern completion and pattern separation in the hippocampus [review]. *Frontiers in Systems Neuroscience*, *7*(74), 1–21. https://doi.org/10.3389/fnsys.2013.00074

Satpute, A. B., & Lindquist, K. A. (2019). The default mode network's role in discrete emotion. *Trends in Cognitive Sciences*, *23*(10), 851–864. https://doi.org/10.1016/j.tics.2019.07.003

Schlichting, M. L., Mumford, J. A., & Preston, A. R. (2015). Learning-related representational changes reveal dissociable integration and separation signatures in the hippocampus and prefrontal cortex. *Nature Communications*, *6*(1), 8151. https://doi.org/10.1038/ncomms9151

Seidemann, R., Duek, O., Jia, R., Levy, I., & Harpaz-Rotem, I. (2021). The reward system and post-traumatic stress disorder: Does trauma affect the way we interact with positive stimuli. *Chronic Stress*, *5*, 1–11. https://doi.org/10.1177/2470547021996006

Suarez-Jimenez, B., Zhu, X., Lazarov, A., Mann, J. J., Schneier, F., Gerber, A., Barber, J. P., Chambless, D. L., Neria, Y., Milrod, B., & Markowitz, J. C. (2020). Anterior hippocampal volume predicts affect-focused psychotherapy outcome. *Psychological Medicine*, *50*(3), 396–402. https://doi.org/10.1017/S0033291719000187

Thome, J., Hauschild, S., Koppe, G., Liebke, L., Rausch, S., Herzog, J. I., Müller-Engelmann, M., Steil, R., Priebe, K., Hermans, D., Schmahl, C., Bohus, M., & Lis, S. (2018). Generalisation of fear in PTSD related to prolonged childhood maltreatment: An experimental study. *Psychological Medicine*, *48*(13), 2223–2234. https://doi.org/10.1017/S0033291717003713

Weaver, S. S., Kroska, E. B., Ross, M. C., Sartin-Tarm, A., Sellnow, K. A., Schaumberg, K., Kiehl, K. A., Koenigs, M., & Cisler, J. M. (2020). Sacrificing reward to avoid threat: Characterizing PTSD in the context of a trauma-related approach-avoidance conflict task. *Journal of Abnormal Psychology*, *129*(5), 457–468. https://doi.org/10.1037/abn0000528

Webler, R. D., Berg, H., Fhong, K., Tuominen, L., Holt, D. J., Morey, R. A., Lange, I., Burton, P. C., Fullana, M. A., Radua, J., & Lissek, S. (2021). The neurobiology of human fear generalization: Meta-analysis and working neural model. *Neuroscience and Biobehavioral Reviews*, *128*, 421–436. https://doi.org/10.1016/j.neubiorev.2021.06.035

Whitfield-Gabrieli, S., & Nieto-Castanon, A. (2012). Conn: a functional connectivity toolbox for correlated and anticorrelated brain networks. *Brain Connectivity*, *2*(3), 125–141. https://doi.org/10.1089/brain.2012.0073

Yassa, M. A., & Stark, C. E. L. (2011). Pattern separation in the hippocampus. *Trends in Neurosciences*, *34*(10), 515–525. https://doi.org/10.1016/j.tins.2011.06.006

Zandvakili, A., Barredo, J., Swearingen, H. R., Aiken, E. M., Berlow, Y. A., Greenberg, B. D., Carpenter, L. L., & Philip, N. S. (2020). Mapping PTSD symptoms to brain networks: A machine learning study. *Translational Psychiatry*, *10*(1), 195. https://doi.org/10.1038/s41398-020-00879-2

Zilcha-Mano, S., Zhu, X., Suarez-Jimenez, B., Pickover, A., Tal, S., Such, S., Marohasy, C., Chrisanthopoulos, M., Salzman, C., Lazarov, A., Neria, Y., & Rutherford, B. R. (2020). Diagnostic and predictive neuroimaging biomarkers for posttraumatic stress disorder. *Biological Psychiatry. Cognitive Neuroscience and Neuroimaging*, *5*(7), 688–696. https://doi.org/10.1016/j.bpsc.2020.03.010

Zou, Q., Ross, T. J., Gu, H., Geng, X., Zuo, X. -N., Hong, L. E., Gao, J. -H., Stein, E. A., Zang, Y. -F., & Yang, Y. (2013). Intrinsic resting-state activity predicts working memory brain activation and behavioral performance. *Human Brain Mapping*, *34*(12), 3204–3215. https://doi.org/10.1002/hbm.22136

SUPPORTING INFORMATION

Additional supporting information can be found online in the Supporting Information section at the end of this article.

How to cite this article: Keefe, J. R., Suarez-Jimenez, B., Zhu, X., Lazarov, A., Durosky, A., Such, S., Marohasy, C., Lissek, S., & Neria, Y. (2022). Elucidating behavioral and functional connectivity markers of aberrant threat discrimination in PTSD. *Depression and Anxiety*, 39, 891–901. https://doi.org/10.1002/da.23295